The vector of jaw muscle force as determined by computer-generated three dimensional simulation: A test of Greaves' model

Philip Clausen [a,*], Stephen Wroe [b], Colin McHenry [a,c], Karen Moreno [b], Jason Bourke [b]

[a] School of Engineering, The University of Newcastle, NSW 2308, Australia
[b] School of Biological, Earth and Environmental Sciences, University of New South Wales, Sydney 2052, Australia
[c] School of Environmental and Life Sciences, University of Newcastle, NSW 2308, Australia

ARTICLE INFO

ABSTRACT

We present results from a detailed three-dimensional finite element analysis of the cranium and mandible of the Australian dingo (*Canis lupus dingo*) during a range of feeding activities and compare results with predictions based on two-dimensional methodology [Greaves, W.S., 2000. Location of the vector of jaw muscle force in mammals. Journal of Morphology 243, 293–299]. Greaves showed that the resultant muscle vector intersects the mandible line slightly posterior to the lower third molar (m3). Our work demonstrates that this is qualitatively correct, although the actual point is closer to the jaw joint. We show that it is theoretically possible for the biting side of the mandible to dislocate during unilateral biting; however, the bite point needs to be posterior to m3. Simulations show that reduced muscle activation on the non-biting side can considerably diminish the likelihood of dislocation with only a minor decrease in bite force during unilateral biting. By modulating muscle recruitment the animal may be able to maximise bite force whilst minimising the risk of dislocation.

Crown Copyright © 2008 Published by Elsevier Ltd. All rights reserved.

1. Introduction

Using traditional two-dimensional (2D) approaches Greaves (1983, 1985, 1988, 2000, 2002) has developed several idealised models of the mammalian mandible that provide insights into mammalian feeding mechanics. Areas explored in these influential works include the relationship between feeding behaviours, the attachment positions of various jaw muscle groups, and their relative strengths. Some outcomes of Greaves' works have been supported by biological data as well as "common sense" mechanics arguments. Until now, however, few detailed three-dimensional (3D) analyses have examined any of these hypotheses.

In recent years finite element (FE) analysis has been widely applied to investigate aspects of cranial mechanics in both living and extinct taxa (Dumont et al., 2005; Rayfield et al., 2001; Rayfield, 2007; Wroe et al., 2007; McHenry et al., 2007). The growing popularity of FE analysis in the modelling of bio-structures has been fuelled by advances in the capability, speed and ease of use of both FE and imaging softwares, the latter used to convert computed tomography (CT) X-ray scan data into detailed and geometrically accurate 3D models. Consequently,

biomechanical questions that were previously investigated using empirical arguments with many simplifying assumptions can now be addressed far more precisely.

Here we use FE modelling of the complete skull of a relatively generalised carnivoran, *Canis lupus dingo*, to explore bite force at eight bite points along the tooth row for both unilateral and bilateral bites; the temporomandibular joint (TMJ) reaction force for the above, and TMJ reactions when the muscles on the non-biting side of the mandible fire sub-maximally. As a broader aim, we evaluate Greaves' argument that dislocation of the mammalian mandible will result during specific hypothetical feeding behaviours (Greaves, 2000). This analysis of the dingo can serve as a starting point for comparative investigations, which will test the generality of Greaves' results for other mammalian taxa.

2. Method

Modelling was based on a 3D heterogeneous FE model of the cranium and mandible of a dingo created by Wroe et al. (2007). In summary surface models were created from computer tomography (CT) of the cranium and mandible with the subsequent solid modelling and analysis done in Strand7 FE software. For the present study, this model was modified and used for the work described in this paper. The FE model consisted of ~900,000 four-node tetrahedral 3D "brick" elements, with muscle forces simulated using pretensioned truss FE (beam FE capable of transmitting axial load only). We manually replaced the pretensioned truss elements with forces acting directly upon nodes. As in Wroe et al., the TMJ was modelled using a hinged beam linked to the cranium and mandible, with the

* Corresponding author at: Mechanical Engineering, School of Engineering, The University of Newcastle, University Drive, Callaghan, NSW 2308, Australia.
Tel.: +61 2 4921 6202; fax: +61 2 4921 6946.
E-mail address: Philip.clausen@newcastle.edu.au (P. Clausen).

axis of this hinge beam oriented to facilitate the interpretation of the mandible joint reaction forces. The analysis was done for two gape positions: near-closed, and for a gape of about 40° (Fig. 1).

For all loading scenarios considered here the model was restrained via a framework of stiff beam elements on the occipital condyle, with one node on this framework restrained for all three translations and rotations. Bite points on the cranium and mandible were simulated by restraining nodes on teeth in the circumferential direction of a cylindrical coordinate system aligned with the axis of the hinge beam. This created a model that could simulate biting and was least restrictive during any bite simulation, but was sufficiently restrained to prevent

Fig. 1. Finite element models of the dingo for (a) near-closed gape and (b) 40° gape. The axis system shown is for the beam finite element used to model the temporomandibular joint. This beam has three axes; the first and second are indicated on the figure, the third axis is normal to the plane of the figure as shown.

rigid body motion. To avoid artificial stress singularities at bite points, the surface region at and around each bite point was tessellated with stiff beams to distribute loading more evenly.

A total of 16 restraint cases were considered for each model. These covered both bilateral and unilateral biting simulations. We applied restraints to the upper and lower canines to the second upper molar (M2) and third lower molar (m3), with each bite point coinciding approximately with the centre of a tooth. The joint reaction force, determined from the end force of the hinge beam, was found for each of the biting positions. Initially, for each bite position we assumed that all jaw adductors were fully recruited to allow direct comparison with the results of Greaves (2000). We then explored the effects on both the bite force and mandible joint reaction when the non-biting side muscles were recruited at 80% and 90% of the maximum value.

Fig. 1a and b shows the TMJ beam axis system for the near-closed gape and open gape simulations respectively. The beam used to simulate the hinge axis has a local coordinate system (in FE modelling nomenclature) that requires three orthogonal axes, which were defined thus: the 3-axis was aligned along the joint axis; the 2-axis is orientated so as to pass through the mid-plane (approximately equivalent to the transverse plane of the skull) of both the cotylar facet and the condylar head; the 1-axis is orthogonal to the 2 and 3 axes with its direction defined by the right hand rule. The direction of the 2-axis was selected such that movement in the negative 2-axis direction would be free of interference from the surrounding bone and therefore the most likely direction for dislocation to occur. Consequently the precise orientation of the beam axis system differs between 40° open and near-closed gapes as shown in Fig. 1.

To directly compare our results with those of Greaves (2000), the magnitude and direction of the jaw muscle vector was determined from the FE model. Greaves assumed that this vector intersected the tooth row just behind m3 at about 30% of the mandibular length from the joint hinge (where the length is measured from the mandible joint hinge to the incisor) measured perpendicular to this muscle vector. From the finite element model, however, it is relatively easy to determine the resultant jaw muscle vector, however, it is more difficult to directly determine the effective lever arm. Here we determined the effective lever arm indirectly by equating moments about the hinge axis from the bite point forces with the moments supplied by the muscles.

3. Results

Fig. 2 shows the bilateral and unilateral bite force for both the near-closed gape and 40° open gape. The bite force is higher for the near-closed gape than for the 40° open gape at the same bite points. For the near-closed gape, the bite force for the bilateral case was up to 108% of the unilateral case. The bite force per tooth, however, is clearly lower in the bilateral case (two sets of opposing teeth biting) than in the unilateral case (one set of opposing teeth biting). Interestingly the difference between bilateral and unilateral bites was negligible in the open gape simulation. Qualitatively the relationship between bite force and tooth position is in agreement with the theoretical predictions of Greaves (1988).
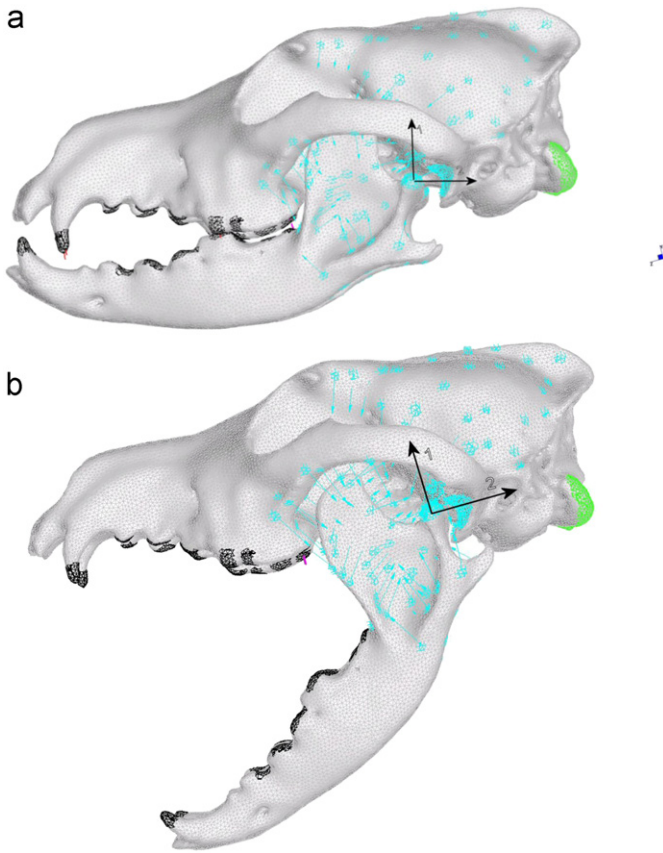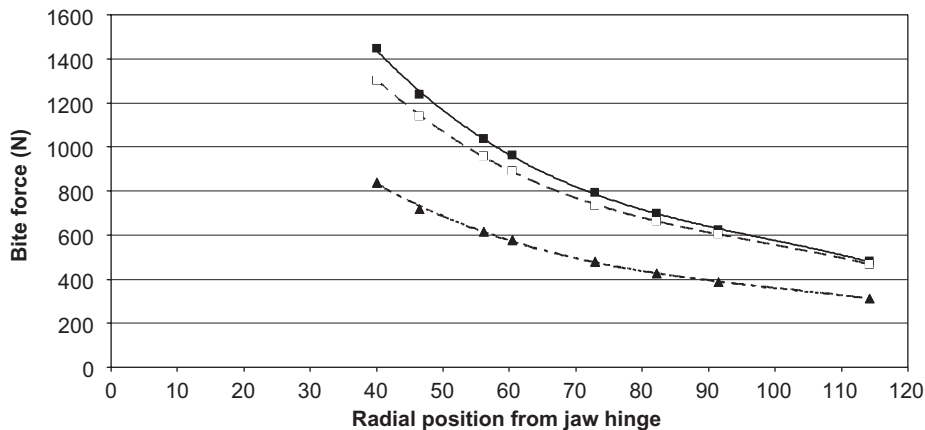

Fig. 2. Bite force for both unilateral and bilateral biting for near-closed and 40° gape. ■—near closed gape simulations and ▲—40° open gape simulation. Shaded symbols are for bilateral bite and open for unilateral bite. Lines shown are of best fit through the data for clarity only.

Table 1
Effective lever arm for the resultant muscle vector for the near-closed gape (0°) and 40° gape

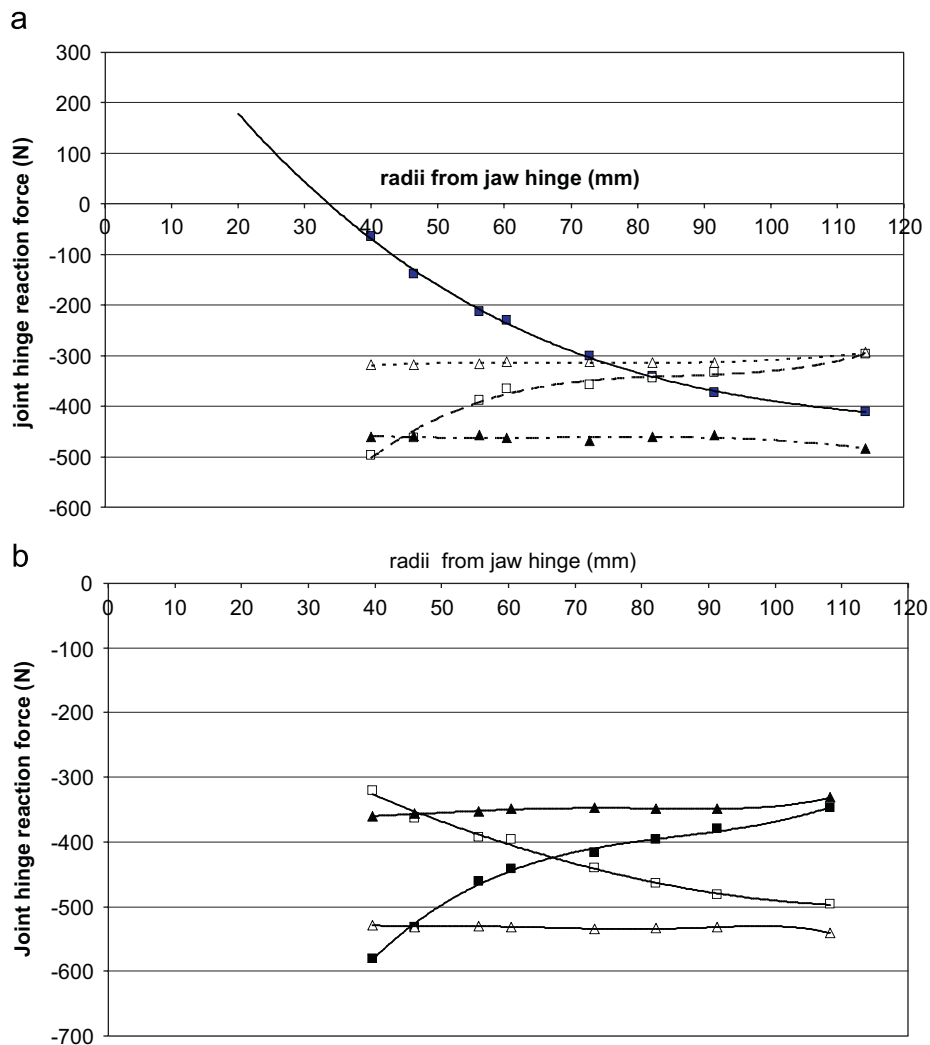| Gape	F_y (N)	F_z (N)	F_{total} (N)	Θ (degs)	Bite moment sum (Nmm)	Effective lever arm (mm)
0°	894.4	−784.4	1189.6	−50.1	26,820	22.5
40°	1166.2	−612.0	1317.0	−62.3	17,375	13.2

Fig. 3. Jaw reaction force on the biting and non-biting side of the mandible for (a) the near-closed gape and (b) the 40° gape. ■—force in the 2-axis direction and ▲—force in the 1-axis direction. Closed symbols are for the biting side and open symbols are for the non-biting side. Lines are of best fit through the data.

Table 1 shows the results of our determination of jaw muscle resultant vectors. Here θ is the angle between the global z-axis (same direction as the 2-axis-direction in Fig. 1b for both models) and the load vector, with a negative angle indicating a posterior direction of the jaw muscle vector. By our method, the jaw muscle vector of the dingo intersects the tooth row line at a radius of 37.6 mm, or when made dimensionless by the mandible length, it intersects at 0.30.

Greaves (1983, 1985, 1988, 2000) developed an empirically based argument identifying the most posterior bite point that would not lead to dislocation of the mandible during feeding. Given the weakness of the TMJ in tension (Spencer and Demes, 1993), for the purposes of this analysis we have deemed a joint to have the potential to dislocate when the joint reaction force in the 2-axis direction (see Fig. 1) approaches zero (i.e., any further decrease will bring the system into tension).

Fig. 3a shows the reaction forces in the joints on the biting and non-biting sides of the mandible during unilateral biting. For all biting positions the reaction force on the joint in the 2-axis direction is negative, which by the system used here, indicates that the joint is in compression and hence has no potential for dislocation. The reaction force is also negative in the 1-axis direction; however, this simply means the mandibular condyle is being forced upwards in contact with the opposing part of the temporal cotyle of the cranium. Extrapolation of the data for the 2-axis direction shows that the joint reaction force is zero at a theoretical bite point of close to 35 mm.

Fig. 3b shows the joint reaction force for both joints under unilateral bites when the dingo has a gape of 40°. Here it is clear that the joint is in compression and will never be in tension, and therefore that the joint will not dislocate during biting.

3.1. Reduced muscle recruitment on balancing side

The results of reduced recruitment on the balancing side, and for maximal muscle firing on both sides of the mandible for unilateral biting are shown in Fig. 4a and b, respectively. Fig. 4a shows that the unilateral bite force diminishes when the muscle recruitment on the non-biting side is reduced, as was expected. The bite force decreased to 92% of the maximum value when the non-biting side muscle recruitment was 80% of maximum, corresponding to a reduction from approximately 1300 to 1200 N in bite force at m3. The results in Fig. 4b show that a reduction in the level of muscle recruitment on the non-biting side increases the compressive force in the biting side joint in the 2-axis direction and reduces the magnitude of the compressive force in the joint on the non-biting side. Extrapolation of this data suggests that by decreasing the muscle recruitment on the non-biting side moves the point posterior of where jaw dislocation on the biting side would have occurred for full muscle recruitment. The biting side joint, therefore, is less likely to dislocate during unilateral biting when the muscle recruitment on the non-biting side has been reduced.

Our results are similar to the predictions of Thomason et al. (1990) for canine anterior bite for the opossum, but whilst their models predicted tension in the biting side TMJ for posterior molar bites (M4), our models suggest that this joint remains in compression for all bite positions including the m3 bite. From our dingo model, the point at which the working side joint would theoretically come under tension is several millimetres posterior of the rear most tooth: Thomason predicts that this point lies anterior of the rear most tooth for the opossum. Given that all the results are predictions based on models rather than in vivo data, there is the opportunity for experimental results to shed further light on this question.

4. Discussion and conclusions

Following the method of Greaves (2000) and using the data in Table 1 (and see Fig. 5), the point of intersection between the jaw muscle resultant and the lower jaw is posterior of the radial position of m3 for this particular mandible, and less than jm3/L ("distance from the projection of the jaw joint (j) to the third
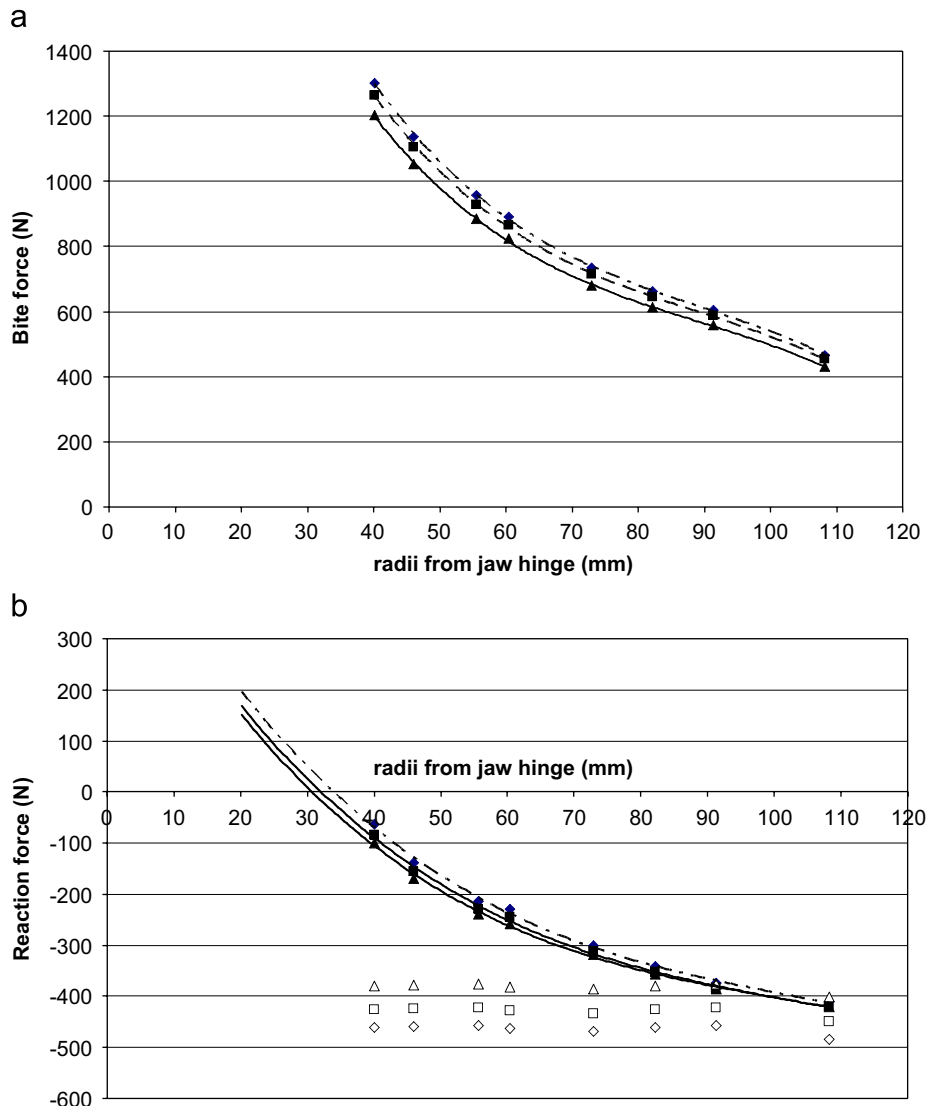

Fig. 4. Bite force (a) and mandible reaction force (b) in the two-direction for the near-close gape for different levels of muscle recruitment on the non-biting side of the mandible. ♦—100% recruitment on non-biting side; ■—90% recruitment on non-biting side; ▲—80% recruitment on non-biting side. Closed symbols are for biting side joint and open symbols are for non-biting side joint. Lines are of best fit through the data.
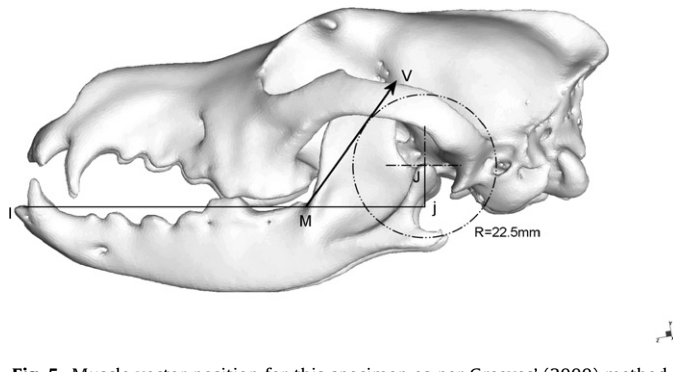
Fig. 5. Muscle vector position for this specimen as per Greaves' (2000) method.

molar divided by the length of the jaw measured for *j* to *I*", Greaves, 2000) for *Canis familiarus* (0.32) from Table 1 of Greaves (2000).

In short, our 3D analyses demonstrate that the dingo is physically unable to bite at a mandible hinge radius of less than 40 mm and therefore incapable of dislocating the biting side of its mandible during ideal unilateral biting, as predicted by the 2D modelling of Greaves (2000). In addition we found that during unilateral biting the joint on the non-biting side of the dingo's mandible is always in compression, with the magnitude of this force remarkably constant with respect to bite point. For bilateral biting, the TMJ is always in compression and therefore the dingo is unable to dislocate its mandible during normal bilateral feeding.

These results also demonstrate that during unilateral biting, moderate 10–20% reductions in applied force on the non-biting side can considerably reduce the likelihood of dislocation on the biting side. In light of this finding we suggest that by controlling levels of muscle recruitment on both the biting and non-biting sides the animal is able to maximise bite force whilst minimising the risk of joint dislocation.

Conflict of interest statement

The work undertaken in this paper is a fundamental nature exploring bite mechanics in a generalised carnivore. As such there is no conflict of interest for any of the authors of this paper.

References

Dumont, E., Piccirillo, J., Grosse, I., 2005. Finite element analysis of biting behaviour and bone stress in the facial skeletons of bats. Anatomical Record 283A, 319–330.
Greaves, W.S., 1983. A functional analysis of carnassial biting. Biological Journal of the Linnean Society 20, 353–363.
Greaves, W.S., 1985. The generalized carnivore jaw. Biological Journal of the Linnean Society 85, 267–274.
Greaves, W.S., 1988. The maximum average bite force for a given jaw length. Journal of Zoology, London 214, 295–306.
Greaves, W.S., 2000. Location of the vector of jaw muscle force in mammals. Journal of Morphology 243, 293–299.
Greaves, W.S., 2002. Modeling the distance between the molar tooth rows in mammals. Canadian Journal of Zoology 80, 388–393.
McHenry, C., Wroe, S., Clausen, P., Moreno, K., Cunningham, E., 2007. Supermodeled sabercat, predatory behavior in *Smilodon fatalis* revealed by high-resolution 3D computer simulation. Proceedings of the National Academy of Sciences 104, 16010–16015.
Rayfield, E., 2007. Finite element analysis and understanding the biomechanics and evolution of living and fossil organisms. Annual Review of Earth and Planetary Sciences 35, 541–576.
Rayfield, E., Norman, D., Horner, C., May-Smith, P., Thomason, J., Upchurch, P., 2001. Cranial form and function in a larger theropod dinosaurs. Nature 409, 1033–1037.
Spencer, M., Demes, B., 1993. Biomechanical analysis of masticatory systems configuration in Neandertals and Inuits. American Journal of Physical Anthropology 91, 1–20.
Thomason, J., Russell, A., Morgeli, M., 1990. Force of biting, body size, and masticatory muscle tension in the opossum *Didelphis virginiana*. Canadian Journal of Zoology 68, 318–324.
Wroe, S., Clausen, P., McHenry, C., Moreno, K., Cunningham, E., 2007. Computer simulation of feeding behaviour in the thylacine and dingo as a novel test for convergence and niche overlap. Proceedings of the Royal Society of London, Series B 274, 2819–2828.